

NATIVE MICRODEFECTS AND AS-GROWN DISLOCATIONS IN PURE AND DOPED InP CRYSTALS

D. Grabco¹, M. Dyntu², and E. Rusu²

¹*Institute of Applied Physics, Academy of Sciences of Moldova, Academiei str. 5,
Chisinau, MD-2028 Republic of Moldova. e-mail: grabco@phys.asm.md*

²*Institute of Electronic Engineering and Nanotechnologies "D. Ghitu",
Academy of Sciences of Moldova, Academiei str. 3/3, Chisinau, MD-2028 Republic of Moldova*

(Received 28 February 2011)

Abstract

The fine defect structure (native microdefects and as-grown dislocations) of pure and doped InP crystals are considered. Some kinds of point defects are detected. They are connected with the technology of crystal growth and impurity concentration. It is shown that the type and concentration of doping impurity essentially change the as-grown dislocation density and influence the mobility of freshly generated dislocations. The mechanism of plastic deformation under the action of a concentrated load is related to dislocation mobility in the InP crystals and impurity type.

1. Introduction

Pure and doped InP crystals are very widely used in modern microelectronics as a substrate for the production of microwave and for optoelectronic devices [1-7]. The quality of fabricated devices essentially depends on the density of point and linear defects in crystals. Crystals with a low density of both linear (dislocations) and point (vacancies, interstitial atoms, fine-dispersed segregations, etc.) defects are most valuable. The perfection of the InP crystal structure is usually reached by doping with various impurities [8-10]. In dependence on the growth conditions, the type and concentration of impurity, it is possible to prepare the InP single crystals with low density of as-grown dislocations and microdefects. However, the fabrication of crystals with low defect density does not resolve all problems of their practical use.

It is known that the materials and devices on its base are subjected to the influence of different external factors in the process of their fabrication and exploitation. These are non-uniform mechanical tensions, temperature fluctuations, irradiation, etc., which are able to create new defects in the crystals. Hence, the quality of devices and instruments will depend not only on the perfection of the as-grown crystal structure, but also on the crystal resistance to the formation of new defects.

Until now there is no clear conception relative to the InP crystal structure perfection (or imperfection), the type of doping impurity and its resistance to deformation under the action of external loads. In accordance with the data reported in [11], the critical stress of dislocations arising owing to uniaxial loading (τ_{cr}) characterizes stability of crystals in regard to affecting stresses and may be used as a comparative criterion for the evaluation of the crystal structure perfection. For instance, the authors of [10] have shown that the critical stress (τ_{cr}) in the A^3B^5 crystals $\tau_{cr} \approx 10\tau_y$, where τ_y is the crystal yield stress.

However, the realization of an experiment of uniaxial loading is associated with a high

number of technical difficulties, special requirements for the dimension of samples under test, etc. In addition, under real conditions, the crystals are commonly subjected to complicated, non-uniform pressures. Thus, another parameter, namely the γ value, is proposed in works [12-14] for the estimation of crystal lattice resistance. The γ parameter is the mobility of dislocation ensembles appearing in the deformed zone under the action of concentrated load, in particular, under microindentation.

An analysis of the defect structure, the type and concentration of doping impurity, the investigation of their influence on the plastic deformation peculiarities will result in a more profound understanding of the hardening mechanism owing to the doping of semiconductor materials. The obtained data, in turn, will contribute to the design of more perfect semiconductor devices.

In this connection, the investigation of the pattern of the defect structure of pure and doped InP crystals and the estimation of the impurity contribution in the deformation regularities under microindentation are considered in the work.

2. Experimental

The researches were fulfilled for pure and doped liquid-encapsulation-Czochralski-grown InP crystals. Doping was made using Sn (donor), Zn (acceptor), Fe (semi-insulating) and Ga (isovalent) elements as impurities. Joint doping with ZnO and Zn:Ga complexes was also performed. The experiments were carried out on the (100) and (111)B planes. The specimens were subjected to the etch-pit technique in order to reveal the fine defect structure. A solution (0.01N CrO₃+30 ml HCl) was used as a selective chemical etcher. Etching time varied from 5 to 10 s. The crystals were preliminary degreased in boiling isopropyl alcohol or toluol and then polished in the bromine-methanol to eliminate the surface oxide film. A study of the fine defect structure (point defects, microdefects, and dislocations) was performed using both scanning electron and light microscopy.

The crystals were deformed by a concentrated load using a PMT-3 microhardness tester (microindentation and sclerometric method) to evaluate the mobility (γ) of fresh dislocation ensembles. A diamond Vickers pyramid was used as the indenter. The applied load (P) varied from 0.1 to 0.4 N. The measurements were performed for two orientations of the indenter on each of the investigated planes: the diagonals d of the indentations parallel to $\langle 100 \rangle$ direction and $d \parallel \langle 110 \rangle$ for the (100) plane and $d \parallel \langle 112 \rangle$ directions for the (111) plane, respectively.

Deformed crystals were subjected to annealing during 2 h at $T = 650$ K. After that, the crystals were again etched to reveal the dislocation structures around the indentations and scratches. Parameters $\gamma = l/d$ and $\gamma_s = l_s/b$ were accepted as characteristics of the dislocation ensemble mobility [13]. Here l is the maximal dislocation removal from the indentation center; l_s is the maximal dislocation removal from the central line of the scratch; d is the indentation diameter, and b is the scratch width.

3. Results and discussion

The data of selective chemical etching illustrated that the pure and doped InP crystals differ in the as-grown dislocation density and the amount and type of point and microdefects. For example, a top view of the surfaces with as-grown dislocations revealed by the etch-pit technique on the (100) and (111) planes is presented in Fig. 1.

The average density of as-grown dislocations in pure InP crystals was $N_D \approx 5 \cdot 10^4 \text{ cm}^{-2}$. The doping with various impurities up to different concentrations enlarged the range of dislocation density (Fig. 2). It is important that each of the used impurities at a definite concentration allows to derive higher perfection of InP structure and to obtain the essential decrease of dislocation density. The lowest dislocation density was achieved by doping with Fe and Zn elements ($N_D \approx 2.5 \cdot 10^3 \text{ cm}^{-2}$). A less effect was revealed for the crystals doped with the Ga isovalent impurity. Nearly dislocation-free InP crystals were obtained using Zn as impurity.

According to the type and concentration of native point and microdefects, the investigated crystals were characterized as follows (Fig. 3, see also Fig. 1). A hardly visible point background with low density ($\sim 10^2 \text{ cm}^{-2}$) occurs on the (100) surface of InP:Sn and pure InP crystals (Fig. 3a and Figs. 1a, 1b; table, points 1, 2). A similar point defect structure appears at some impurity concentrations on the (111) surfaces of InP:ZnO (Table, point 1, 2) and InP:Zn:Ga.

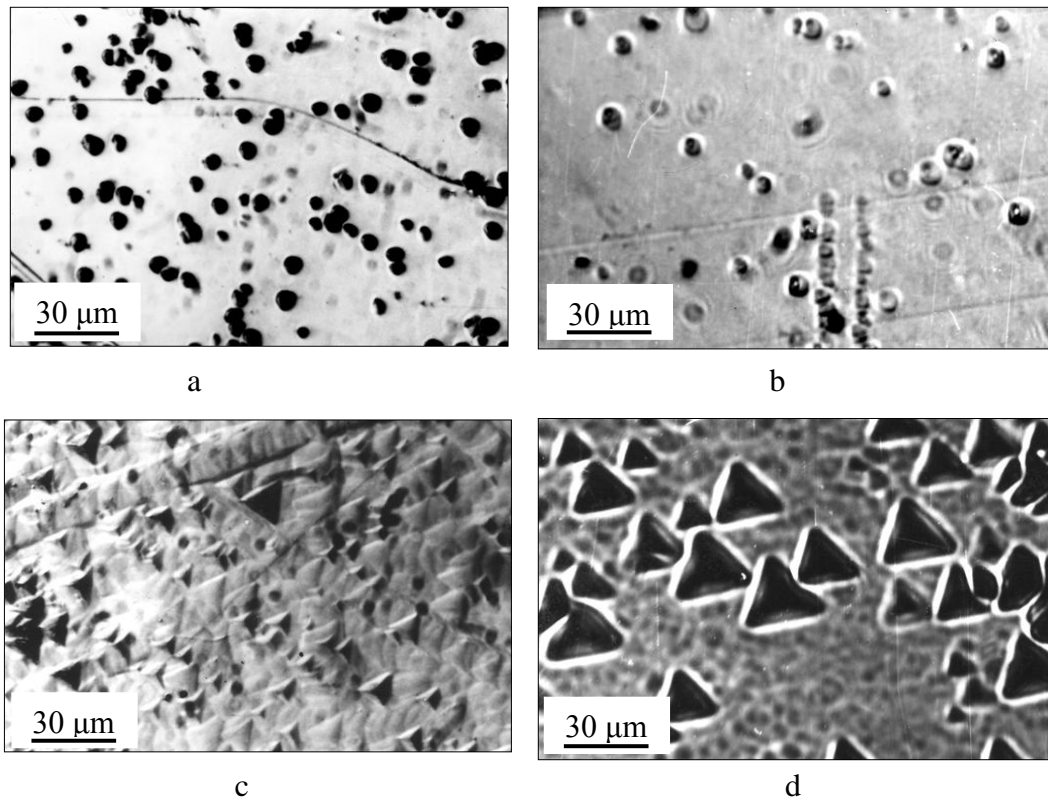


Fig. 1. As-grown dislocations on the (100) (a, b) and (111) (c, d) planes of pure and doped InP crystals: (a) InP (pure); (b) InP:Sn; (c) InP:Ga; and (d) InP:ZnO;

Weak-point background with intermediate density ($\sim 10^3$ - 10^4 cm^{-2}) is specific to the InP:ZnO and InP:Fe crystals (Figs. 1d, 3b; table, points 4, 5). Cellular or triangular microdefects with medium size ($\sim 15 \mu\text{m}$) and high density ($\sim 10^5$ - 10^6 cm^{-2}) and larger microdefects ($\sim 25 \mu\text{m}$) with fairly high density are characteristic of crystals InP:Zn, InP:Ga (Figs. 3c, 1c; table, point 6) and InP:Fe crystals (Fig. 3d; table, point 7), respectively. Very large microdefects (~ 100 - $150 \mu\text{m}$) were also observed at some concentration of Zn, Sn, and Fe impurities (table, points 8-10; Figs. 3e, 3f).

We suppose that this variety of microdefects is due to the formation of intrinsic In_i (interstitial indium) point defects in the isolated state and in the associated one, as well as Frenkel's defects, precipitations, etc. This assumption is in agreement with the results obtained in

[9, 10, 14, 15]. So, the authors of [9, 10] found that the doping of InP crystals with various impurities is accompanied by a change in the lattice parameter (a): donor impurities (S, Ge) lead to an increase in the lattice period, and acceptor ones (e.g., Zn) lead to its decrease. The lattice period is monotonically increased because of the increase in the donor impurity concentration. It is associated with the fact that a donor impurity causes narrowing while an acceptor impurity extends the low temperature limit of the InP homogeneity range ($T > 950^{\circ}\text{C}$). The narrowing leads to the intensification of the decay processes of the (InP:S, Ge) solid solution and to the generation of the great number of Frenkel's defects ($\text{In}_i + \text{V}_{\text{In}}$) at the initial stage, which anomalously enlarge the lattice period.

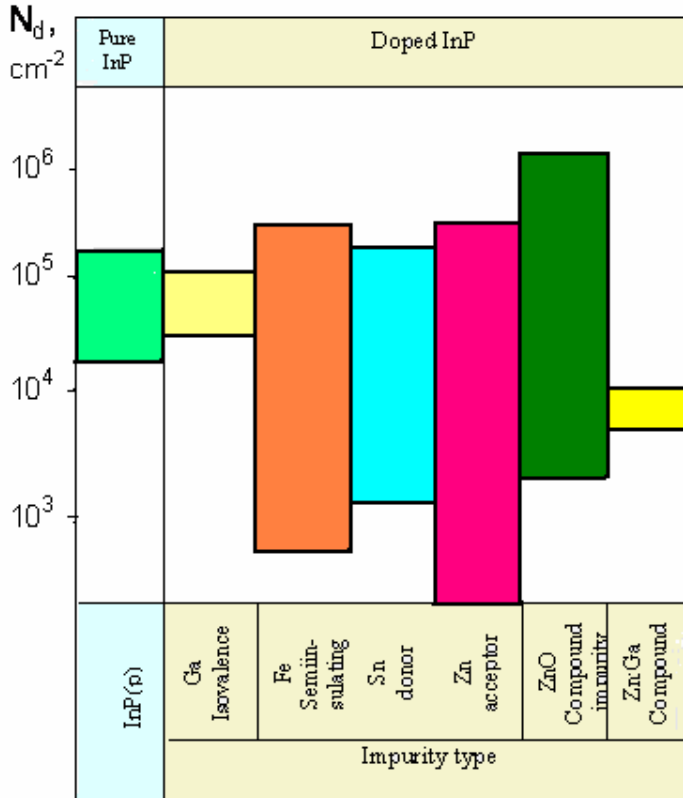


Fig. 2. Density intervals of as-grown dislocations in pure InP crystals and the ones doped with various impurities

In the case of Zn acceptor impurity, a decreases with increasing Zn concentration according to the Vegard's law, which appear to hold for comparatively small concentrations (<1 at %). The concentration of Zn in InP crystals essentially increases if the doping grade becomes high enough. This leads to the formation of fine-dispersed segregations enriched by the excess of In atoms for both the donor and acceptor impurities (see Figs. 3e, 3f and table, pp. 9-11).

The investigation of A^3B^5 compounds also showed [15] that the doping with donor impurities intensifies the decay of the solid solution oversaturated by the basic component with the creation of interstitial atoms and vacancies; that is, there is an abnormally high concentration of superfluous intrinsic interstitial atoms, which are condensed after thermal processing.

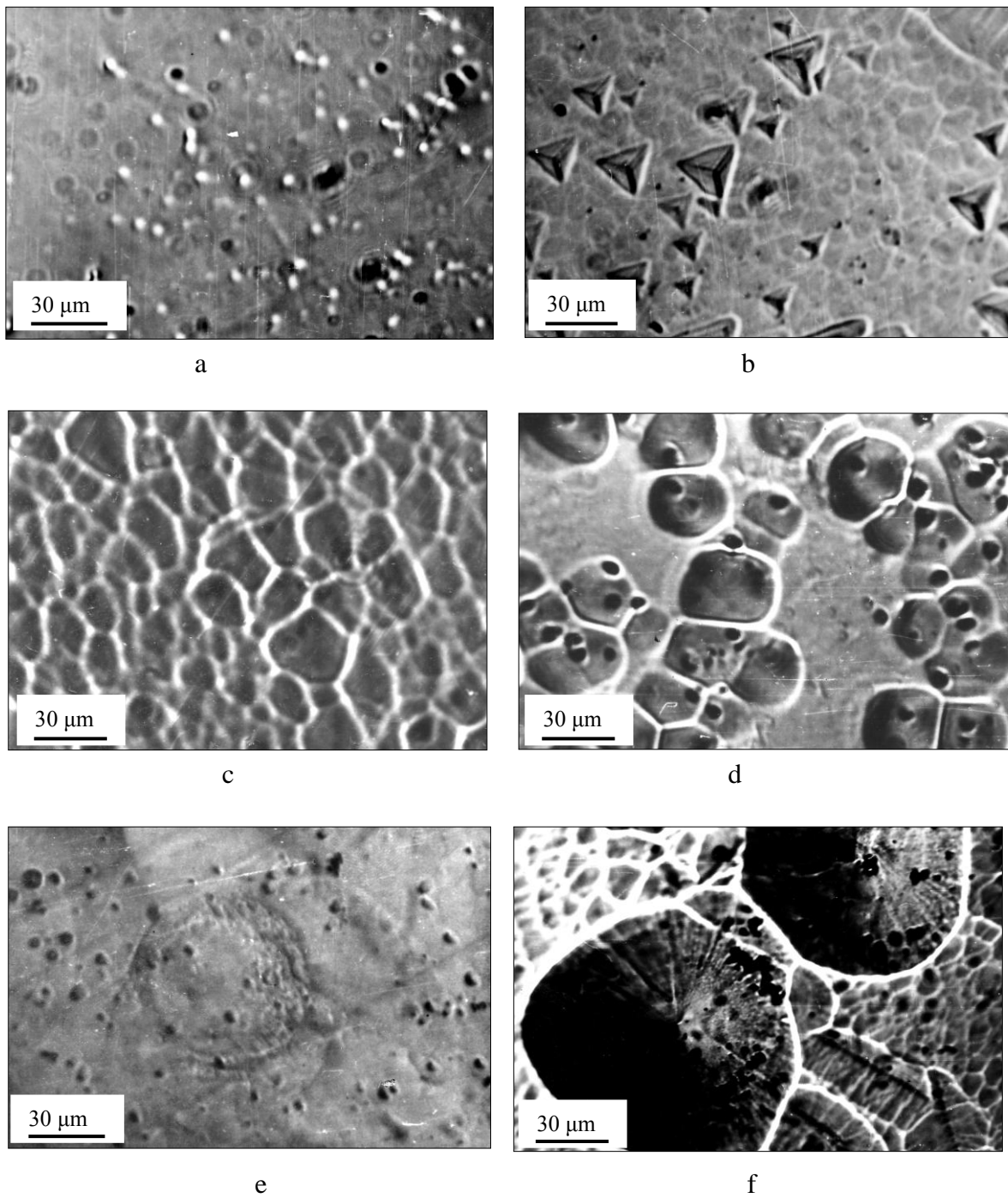


Fig. 3. Native microdefects on the (100) (a, d, e) and (111) (b, c, f) planes of pure and doped InP crystals: (a) InP (pure); (b) InP:ZnO; (c) InP:Zn; (d) InP:Fe; (e) InP:Sn; and (f) InP:Zn.

Main electrical and plastic parameters of pure and doped InP crystals

No	Crystal	Plane	Carrier density, n , cm^{-3}	Carrier mobility, μ , $\text{cm}^2/\text{V}\cdot\text{s}$	As-grown dislocation density, N_D , cm^{-2}	Defect type and pattern of native point and microdefects	Features of zones deformed under the action of concentrated loads and 2-h annealing at 650K
1	InP (pure)	(100)	$4.1 \cdot 10^{16}$	3900	$(2-3) \cdot 10^4$	I. Hardly visible point background with very low density	Middle dislocation zone and twins $\gamma=2\div 4$; $\gamma_s=2\div 4$;
2	InP:Sn	(100)	$9.2 \cdot 10^{17}$	-	$5 \cdot 10^3 - 1 \cdot 10^4$		Well-grown dislocation zone $\gamma=4\div 6$; $\gamma_s=4\div 6$;
3	InP:Zn O	(111)	$5.6 \cdot 10^{18}$	46	$(1.5-3) \cdot 10^4$		Large dislocation zone $\gamma>6$; $\gamma_s>6$
4	InP:Zn O	(111)	$7.0 \cdot 10^{17}$	90	$(5-8) \cdot 10^3$	II. Weak-point background with intermediate density	Large dislocation zone $\gamma>6$; $\gamma_s>6$
5	InP:Fe	(100)	-	-	-		Well-grown dislocation zone and twins $\gamma=4\div 6$; $\gamma_s=4\div 6$;
6	InP:Zn	(111)	$6.0 \cdot 10^{17}$	80	$(2-3) \cdot 10^4$	III. Microdefects with middle dimension and high density	Very small dislocation zone and long and dense twins $\gamma<1$; $\gamma_s<1$;
7	InP:Fe	(100)	$2.67 \cdot 10^9$	530	$(2-3) \cdot 10^4$	IV. Large microdefects with middle dimension and enough high density	Well-grown dislocation zone and twins $\gamma=4\div 6$; $\gamma_s=4\div 6$;
8	InP:Zn	(100)	$2.7 \cdot 10^{18}$	50	$2 \cdot 10^3 - 8 \cdot 10^3$	V. Very large microdefects with low density	Small dislocation zone and twins $\gamma=1\div 2$; $\gamma_s=1\div 2$;
9	InP:Sn	(100)	$9.8 \cdot 10^{17}$	-	$1 \cdot 10^4$		Middle dislocation zone $\gamma=2\div 4$; $\gamma_s=2\div 4$;
10	InP:Fe	(100)	$2.07 \cdot 10^8$	325	$3 \cdot 10^3 - 1 \cdot 10^4$		Middle dislocation zone $\gamma=2\div 4$; $\gamma_s=2\div 4$;

Thus, the analysis of the fine defect structure in InP crystals demonstrated a wide variety of both the linear defect density (as-grown dislocations) and the type and concentration of point defects and microdefects. The question arises, how will all this diversity of crystal imperfections influence the material behavior under the action of a concentrated load?

To this end, we studied the pattern of the deformed zones near the indentations and scratches and estimated the mobility of dislocations, the main bearers of plasticity. It is known [13, 14] that the crystal strength (or hardness) is closely connected with the mobility of freshly generated dislocations. The hard materials are characterized, as a rule, by low dislocation mobility. The dislocation mobility is usually high in soft crystals. Note that this regularity signifies if the crystals are deformed by the mechanism of dislocation plasticity. At present, the alternative deformation mechanisms (twinning, interstitial, phase transition, etc.) are known. They can replace the dislocation mechanism if the latter is retarded. Nevertheless, other mechanisms need, as a rule, greater external forces for realization of the plastic deformation than the dislocation mechanism.

Thus, both the decrease of the dislocation mobility and implication of other plastic deformation mechanisms serve as a sign of the crystal structure hardening of solids.

For the qualitative estimation of the zones deformed by dislocation mobility, we selected five specific groups:

- very small dislocation zone - $\gamma < 1$; $\gamma_s < 1$;
- small dislocation zone - $\gamma = 1 \div 2$; $\gamma_s = 1 \div 2$;
- middle dislocation zone - $\gamma = 2 \div 4$; $\gamma_s = 2 \div 4$;
- well-grown dislocation zone - $\gamma = 4 \div 6$; $\gamma_s = 4 \div 6$;
- large dislocation zone - $\gamma > 6$; $\gamma_s > 6$.

The main parameters of the investigated InP crystals and the features of the deformed zones observed under the action of a concentrated load are presented in the table. The detailed analysis of the table data reveals a certain typical regularity. So, higher density of as-grown dislocations is observed together with less developed dislocation structure near the indentations and scratches in crystals doped with the same impurity (cf., table, pp. 6 and 11 for InP:Zn, or pp. 1 and 10 for InP:Sn). This fact can denote that the high density of as-grown dislocations is one of the hardening factors for the motion of fresh dislocations. Similarly, one can say that microdefects of middle dimensions and high density play a small hardening role (cf., Table, p. 6). According to the table, hardly visible and weak-point background and large microdefects apparently are no real obstacles for the fresh dislocation motion.

We suppose that the type of doping impurity makes a major contribution to the mobility of freshly generated dislocations. In fact, it follows from the table and Fig. 4a that the dislocation zone of the middle dimension and moderate twinning are characteristic of pure InP. Doping with a semi-isolating impurity (Fe) leads to an increase in the dislocation zone and holds the inclination to twinning. The crystals doped with a donor impurity (Sn) are characterized by the well developed dislocation structure and absence of twinning. On the contrary, an acceptor impurity (Zn) hinders the dislocation mobility and activates the crystal tendency to twinning. Figure 4 illustrates a pronounced difference of the deformed zones in dependence on doping impurity type. Really, the deformed zone around the scratches on the (100) plane of InP:Sn crystals has a well-developed dislocation structure without twins (Fig. 4b). On the InP:Zn crystals, the dislocations can be observed only in the close proximity to scratches, the rest deformed zone is formed from the dense rows of twins (Figs. 4 c, 4d).

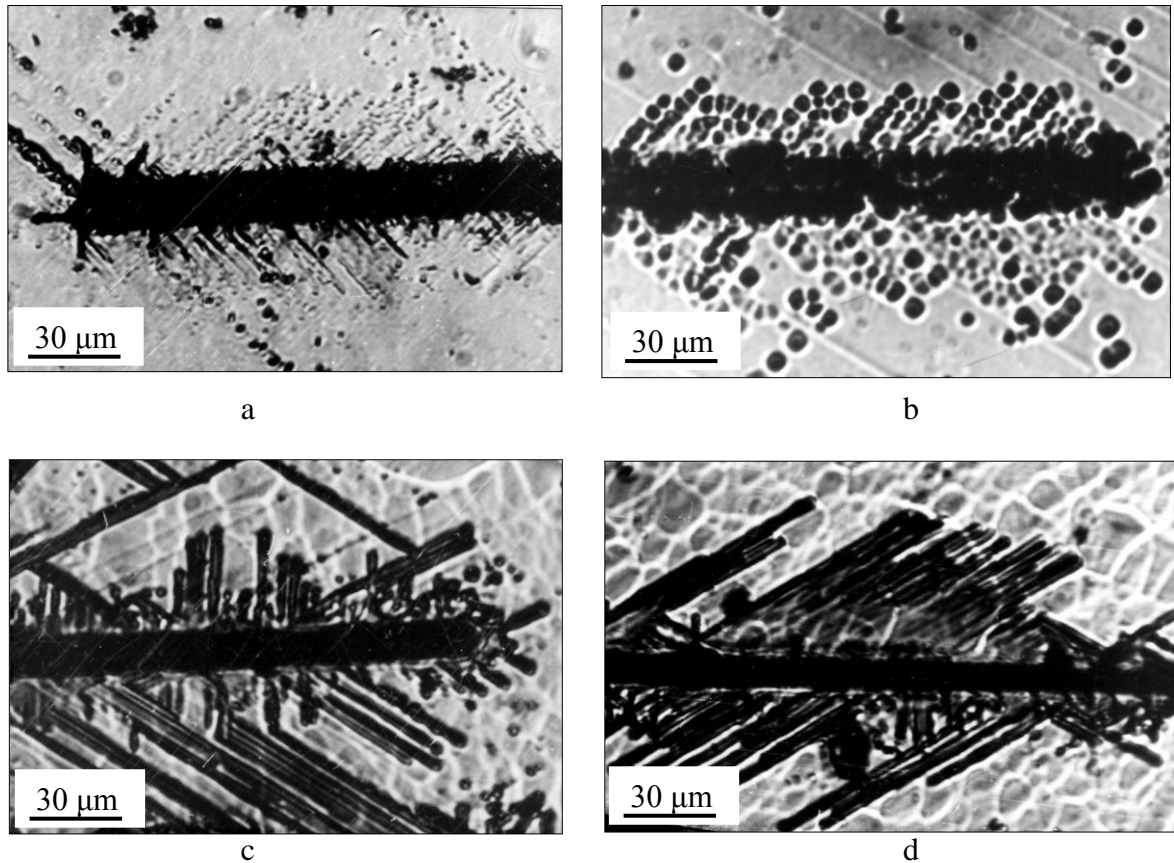


Fig. 4. Dislocation zones and twins around the scratches on the pure and doped InP crystals: (a) pure InP (100); (b) InP:Sn(100); and (c, d) InP:Zn (111).

These data can be explained from the point of view the authors of [9, 10] about the diverse influence of donor and acceptor impurities on the lattice parameter (a) of InP crystals. In fact, if the donor impurity leads to the lattice parameter increase, it is similar to the effect of temperature growth. In accordance with [12-14], the deformation at higher temperature activates the dislocation mobility and reduces the tendency to twinning.

Again, the decrease of lattice parameter caused by acceptor impurity doping will be analogous to the effect of temperature decrease. It will be followed by signs which are specific to this situation, i.e., the reduction of dislocation mobility and the enhancement of the tendency to twinning [13].

The doping of InP crystals with the ZnO complex deserves a particular consideration. In this case, the acceptor impurity (Zn) enters into InP crystal lattice as well, but the results of the study of the deformed zones (Fig. 5) indicate that the plastic deformation occurs more easily.

One can assume that the incorporation of oxygen (simultaneously with Zn) leads to the narrowing of the region of solid solution homogeneity, to the additional transition of In into interstitial sites and, as a result, to an increase in the lattice parameters and plasticity due to the activation of the deformation dislocation mechanism. Supplementary investigations to confirm this assumption are necessary.

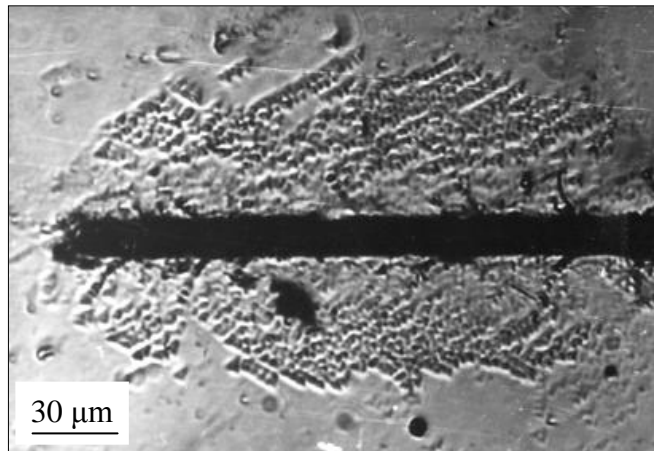


Fig. 5. Dislocation zone around the scratch on the (111) plane of the InP:ZnO crystals.

Note that the dislocation and twinning mechanisms are the main mode of plastic deformation under the action of a concentrated load in the InP crystals both pure and doped. However, the contribution of each of these mechanisms one can change owing to the incorporation of different impurities.

4. Conclusions

The investigation of pure and doped InP crystals showed that impurities lead to a variation in the as-grown dislocation density. By changing of the type and concentration of impurities, one can essentially modify the dislocation density diminishing the N_D values down to $N_D \approx (1-5)10^3 \text{ cm}^{-2}$. Sometimes it facilitates the obtaining of free dislocation crystals.

It is shown that impurities influence the pattern of the native point structure. Some kinds of point and microdefects are detected. The appearance of different types of point and microdefects can be related to the technology of crystal growth and impurity type and concentration.

The mobility of freshly generated dislocations is essentially connected with the type of doping impurity. As a rule, a Fe impurity weakly affects the dislocation mobility, a donor impurity (Sn) increases, and an acceptor impurity (Zn) decreases the dislocation mobility. Point defects, microdefects, and as-grown dislocations weakly influence the dislocation mobility.

The mechanism of plastic deformation in InP crystals under concentrated load action is usually related to dislocation mobility. The dislocation mechanism of plastic deformation is characteristic of crystals that exhibit the high dislocation mobility (InP:Sn, InP:ZnO). The crystals with low dislocation mobility show a higher tendency to twinning (InP:Zn).

Acknowledgments

The authors are grateful to Eng. Maria I. Medinschi for help in some experiments.

References

- [1] Schmidt Handbook Series on Semiconductor Parameters, vol. 1, M. Levinshtein, S. Rumyantsev and M. Shur, ed., World Scientific, London, 1996, pp. 169-190.
- [2] Dargys and J. Kundrotas Handbook on Physical Properties of Ge, Si, GaAs and InP, Vilnius, Science and Encyclopedia Publishers, 1994.
- [3] J. Van Campenhout, P. Rojo-Romeo, P. Regreny, C. Seassal, D. Van Thourhout, S. Verstuyft, L. Di Cioccio, J.-M. Fedeli, C. Lagahe, and R. Baets. Optics Express, 15, 11, 6744, (2007).
- [4] M. Kostrzewa, L. Di Cioccio, M. Zussy, J.C. Roussin, J.M. Fedeli, N. Kernevez, P. Regreny, Ch. Lagahe-Blanchard, and B. Aspar. Sensors and Actuators A: Physical, 125, 2, 411, (2006).
- [5] J.-ichi Echigoya, A. Yamaguchi, E. Aoyagi, Yu. Hayasaka and K. Hiraga. J. Electron Microscopy , 47(6), 621 (1998).
- [6] Indium Phosphide in Semiconductor Electronics, Ed. S.I. Radautsan, Kishinev, "Stiinta", 1988, (in Rus.).
- [7] M.J. Mondry. IEEE, Photonics Tehn. Let., 4, 6, 627, (1992).
- [8] M.S. Hybertsen. SPIE, 2994, 747, (1997).
- [9] A.N. Morozov, E.V. Micriukova, V.G. Bublic, et al. Kristallografiya, 33, 5, 1213, (1988).
- [10] E.V. Mikriukova, A.N. Morozov, A.V. Berkova, et al. Kristallografiya, 33, 5, 1219, (1988).
- [11] N.V. Mejennyi, V.B. Osvenskii, and A.G. Milvidskii. Kristallografia, 35, 5, 1182, (1990).
- [12] Yu.S. Boyarskaya, D.Z. Grabco, and M.P. Dyntu. Cryst. Res. & Techn., 16, 4, 441, (1981).
- [13] D.Z., Grabco, Iu.S. Boyarskaya, and M.P. Dyntu. Mechanical Properties of the Bi Type Semimetals, Kishinev, "Stiinta", 1982, 123p. (in Rus.).
- [14] Iu.S. Boyarskaya, D.Z. Grabco, and M.S. Kats. Physics of Microindentation Processes, Kishinev, "Stiinta", 1986, 293 p. (in Rus.).
- [15] M.G. Milvidskii and V.B. Osvenskii. Structural Defects in the Semiconductor Single Crystals, "Metallurgiya", 1984, 255 p.(in Rus.).